Quantum Electronics **49** (4) 322–329 (2019)

https://doi.org/10.1070/QEL16970

Method for real-time measurement of fluctuations of the ratio of peak power to duration of high-repetition-rate ultrashort pulses

A.V. Andrianov, E.A. Anashkina, M.Yu. Koptev, A.V. Kim

Abstract. **A method is proposed for estimating ratio fluctuations of the peak power to the duration of ultrashort pulses (USPs), based on the measurement of the radiation spectrum nonlinearly broadened in the Kerr medium for only four wavelengths. The method provides a fairly simple measurement processing which can be performed in real time using analogue circuitry even without the digitisation of signals, whereas the operation speed is only limited by the response time of photodetectors and analogue circuits. Numerical studies have shown the possibility of applying the method even for pulses having a substantial asymmetry and containing a significant pedestal. The use of the developed method for analysis of fluctuations of the pulse parameters of a high-power laser system has been experimentally demonstrated, with a short optical fibre section employed for spectrum broadening.**

Keywords: *USP measurement, self-phase modulation, spectrum broadening.*

1. Introduction

Recently, there has been an upsurge of interest in the development of USP laser systems with a sufficiently large peak power and a high repetition rate lying in the megahertz- and higher frequency regions [1]. This is largely due to a high potential of these systems for conducting experiments on nonlinear interaction of laser radiation with matter, for example, on the generation of high harmonics with a fairly large average power, in which a high repetition rate helps accumulate statistics within a short time [2]. The USP lasers with even a higher repetition rate (above 1 GHz) and high stability are of importance for the tasks of metrology and radio-photonics [3, 4]. It is essential to measure in experiments the characteristics of pulses generated by laser systems and resulting from nonlinear interactions [5]. An interesting, but sparsely explored problem in this area is the development of methods for fast evaluation of key pulse parameters (e.g. peak intensity, duration, energy fraction in the pedestal), which could be conducted at high speed, ideally – in real time. In our opinion, a detailed study on the stability of the parameters of USP generated by powerful systems is currently not given enough attention.

Research in this area would be useful in terms of developing high-power laser systems with high energy and average power, for example, actively developing fibre systems with coherent beam summation [6]. A special feature of fibre systems is their strong sensitivity to nonlinear distortions in the process of amplification of a high-power pulse, which requires the development of distortion compensation methods, for example, using feedback systems to control the shape and phase of a pulse on the basis of light modulators. A necessary part of such a system is a scheme for fast diagnostics of the femtosecond pulse shape, and also a scheme for fast (real-time) evaluation of its key parameters (duration and peak intensity).

To date, there are quite a large number of diagnostics methods for ultrashort pulses, based on various principles and nonlinearity types [5]. However, most of them are used in the regime of averaging over many pulses, while the retrieval algorithms are comparatively time-consuming for those methods that can operate in the single-pulse regime.

From the viewpoint of fast measurement of the pulse parameters, in our opinion, there are great prospects for methods based on the observation of spectrum changes during the pulse propagation through a medium with Kerr nonlinearity [7–9]. The peculiarity of these methods is their sensitivity to the peak pulse power, which is manifested in the easily recorded qualitative changes in the broadened spectrum when the power is varied. It should be noted that the most part of indirect approaches to the peak power estimation based on the measurements of pulse energy, its shape, and duration using FROG, autocorrelation, SPIDER, and other methods [5], which may ignore some fundamentally important factors (for example, the presence of a lengthy pulse pedestal), sometimes give distorted peak power data. Therefore, methods based on the Kerr nonlinearity can provide independent peak power estimation: as example, observation of the self-focusing threshold makes it possible to estimate the peak power of high-power fibre systems [10]. Recently, there has been an upsurge of interest in single-pulse measurements for systems operating at a high repetition rate [11, 12].

In most laser systems operating at a high repetition rate, the pulses in a sequence do not differ much from each other. In this case, the averaged characteristics of a pulse, including the shape of the intensity and phase profiles, can be quite easily found by FROG, SPIDER, and similar methods. The fluctuations of the pulse parameters around the mean values are of considerable interest in this case. Undoubtedly, ideally, real-time measurements of the pulse shape and its phase in each pulse would give the most complete information about the system. However, for many applications, information on the key pulse characteristics, such as peak power and duration, would be very useful and sufficient.

In this paper, the possibility of fast real-time measurement of ratio fluctuations of the USP peak power to their duration

A.V. Andrianov, E.A. Anashkina, M.Yu. Koptev, A.V. Kim Institute of Applied Physics, Russian Academy of Sciences, ul. Ul'yanova 46, 603950 Nizhny Novgorod, Russia; e-mail: alex.v.andrianov@gmail.com

Received 19 February 2019
Kvantovaya Elektronika **49** (4) 322–329 (2019)
Translated by M.A. Monastyrskiy

by means of only four-wavelength measurement of fluctuations of the radiation spectrum broadened in the Kerr nonlinear medium is numerically and experimentally studied. The possibility of separate restoration of the peak power and pulse duration, given there is additional information about the pulse, is also discussed.

2. Measurement method

The idea of the method proposed is quite simple and is illustrated in Fig. 1. The radiation under studying passes through a medium with Kerr nonlinearity (for example, a nonlinear fibre), in which the signal spectrum becomes significantly broadened. The broadened spectrum is then recorded for several frequencies by means of fast photodetectors. In using fast photodiodes, this can be done for each pulse in a high-frequency sequence in real-time regime. We further demonstrate that it suffices to measure the spectrum at four frequency points in order to estimate ratio fluctuations of the peak power to the pulse duration around its mean values. To adjust the circuit, it is also desirable to be able to observe the full signal spectrum; however, this can be accomplished using a slow sensor in the regime of averaging over many pulses. In addition, the calibration of measurements requires information about the characteristic shape and duration of a pulse, which can also be extracted from measurements by the FROG or SPIDER methods in the regime of averaging over many pulses.

Let the signal under study be a sequence of pulses with complex-valued pulse amplitude

$$A(t) = |A(t)|\exp[i\varphi(t)]. \tag{1}$$

We assume that the pulse shapes in the sequence are not much different; therefore, we allow for the possibility of fluctuations of all parameters (peak intensity, duration, shapes of phase and envelope). As a result of passing through the Kerr nonlinear medium with the nonlinearity coefficient γ, the pulse experiences self-phase modulation (SPM), so that the complex-valued amplitude $A_{\text{out}}(t)$ at the output takes the form

$$A_{\text{out}}(t) = |A(t)|\exp[i\gamma|A(t)|^2 + i\varphi(t)]. \tag{2}$$

Nonlinear phase modulation contributes to the instantaneous frequency

$$\omega(t) = \frac{\partial}{\partial t}\Big[\gamma|A(t)|^2 + \varphi(t)\Big]. \tag{3}$$

Due to emergence of new frequency components, the spectrum experiences broadening, while the pulse regions for which the instantaneous frequency $|\omega(t)|$ is large make a decisive contribution to the wings of the broadened spectrum. The pulse leading edge makes the main contribution to the low-frequency wing of the spectrum, and the trailing edge – to the high-frequency one (in the case that the nonlinearity has a

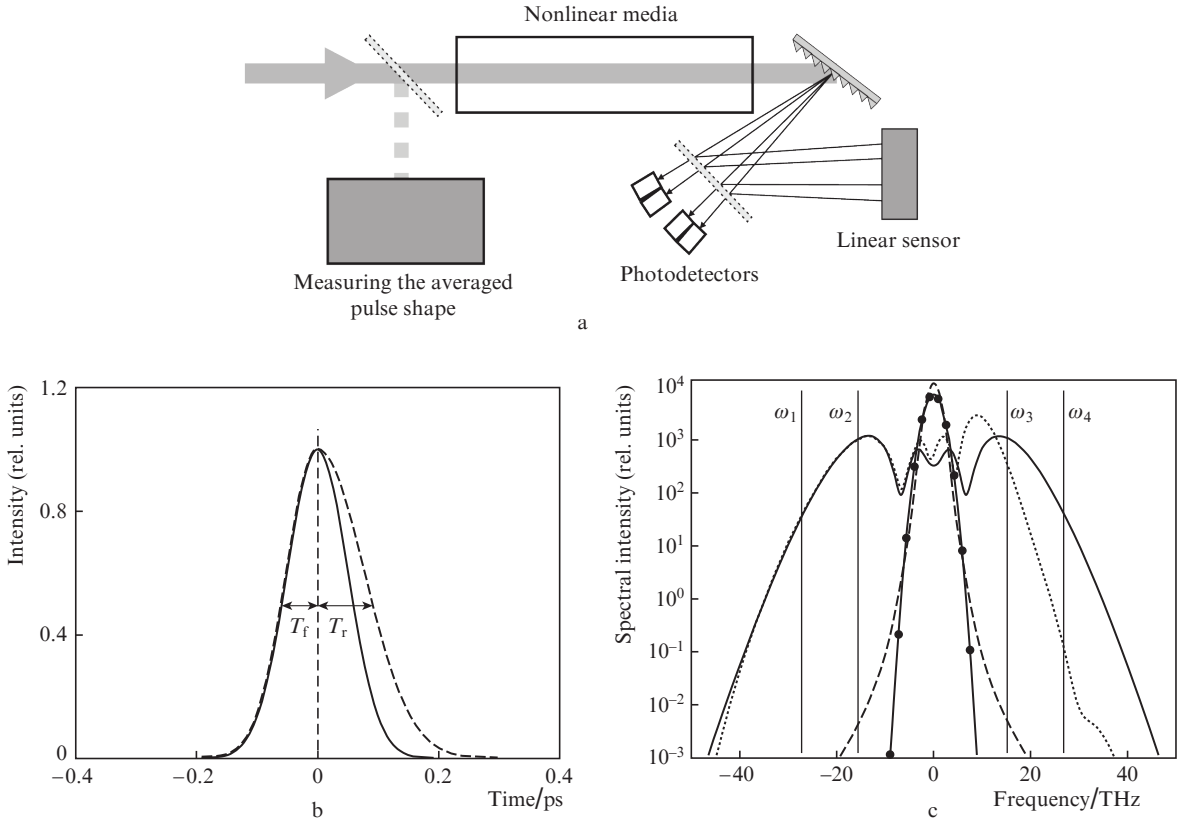

Figure 1. (a) Scheme illustrating the principle of the method for estimation of the pulse characteristics by measuring the broadened spectrum of the pulse under study, (b) symmetric (solid curve) and asymmetric (dashed curve) probe pulses, (c) spectra of symmetric (solid curve with dots) and asymmetric (dashed curve) pulses and also broadened spectra of symmetric (solid curve) and asymmetric (dashed curve) pulses. Vertical lines here and in Fig. 3b indicate the frequencies at which spectral intensity is recorded on the broadened spectrum's wings.

positive sign). Let us make the following assumptions with regard to the input pulse shape and nonlinearity magnitude, which allow us to relate the pulse characteristics to the shape of the broadened spectrum's wings. Suppose that the regions where the instantaneous frequency reaches large (in modulus) values are fairly well localised in time, as is observed for smooth bell-shaped pulses: the maximum and close-to-maximum values of the instantaneous frequency are reached at the pulse fronts. In this case, the lengths of the low-frequency and high-frequency wings of the broadened spectrum are determined mainly by the time derivative of the intensity at the leading and trailing edges of the pulse. This assumption is well fulfilled not only for single-peak pulses, but also for structures containing a single fairly smooth main peak with a sufficiently high intensity and an extended low-intensity pedestal which may have a complex structure with a multitude of local maxima. An undesirable situation is, for example, the presence of dual pulses having the same order of intensity and duration. In this case, both pulses contribute to the spectrum wings, thus making the spectrum strongly modulated.

Then we assume that the derivative of the nonlinear phase significantly exceeds that of the initial pulse phase, which is the case for input pulses close to the transform-limited ones, and at a sufficiently high nonlinearity. In this case, the shape and length of the broadened spectrum's wings are virtually independent of the initial pulse phase and are only determined by its intensity profile. Note that if the pulse is scaled in time, i.e. the amplitude $A(t)$ is replaced by $A(\alpha t)$, its spectrum (both initial and broadened) turns out scaled in wavelengths: the spectrum $S(\omega)$ changes to $S(\omega/\alpha)$. Now it is possible to put forward a hypothesis that variations in the shape of wings in the broadened spectrum stipulated by variations in the pulse shape and peak power are mainly determined by variations in the ratio P_{peak}/T, where P_{peak} is the peak power, and T is the pulse duration.

As a value characterising the shape of the wings in the broadened spectrum and being quite easily measured in experiment, we use a ratio of spectral intensities taken at two frequency points in the low-frequency and high-frequency wings of the spectrum: $s_{\text{L}} = S_1/S_2$ and $s_{\text{H}} = S_4/S_3$, where S_{1-4} are the spectral intensities taken at four frequency points (Fig. 1c). With allowance for the hypothesis we have put forward and possible pulse asymmetry, these relations are determined by the time derivatives of intensity at the leading and trailing edges of the pulse, or, approximately, by the ratios $P_{\text{peak}}/T_{\text{f}}$ and $P_{\text{peak}}/T_{\text{r}}$, where T_{f} and T_{r} are characteristic durations of the leading and trailing edges, respectively. The total pulse duration is $T \approx T_{\text{f}} + T_{\text{r}}$. If the pulse shape fluctuates within small limits, the fluctuations of the values $P_{\text{peak}}/T_{\text{f}}$ and $P_{\text{peak}}/T_{\text{r}}$ can be uniquely related to the fluctuations of the measured ratios s_{H} and s_{L}. The function that determines this relationship can be found in numerical simulations based on the approximately measured pulse shape. After that the P_{peak}/T ratio can be measured very fast (in fact, in real-time regime) using data from only four single-element photodetectors.

3. Numerical simulation

To verify the applicability of the proposed method, we performed numerical experiments in which we tried to simulate a situation typical of a real experiment. A Gaussian pulse was chosen as the probe pulse. We assumed that the spectrum broadening occurred within a short segment of nonlinear medium, so we neglected the dispersion effects and took into account only the instantaneous Kerr nonlinearity. It was also assumed that the nonlinearity was sufficiently high (B-integral was equal to ~ 10); therefore, the spectrum broadening was rather strong (Fig. 1). The spectrum had a shape characteristic of SPM: an oscillating structure was observed, in which the number of peaks increased with increasing nonlinearity. As reference points in the spectrum, at which the spectral intensity should have been measured, two points on the high-frequency and low-frequency wings of the pulse were selected, corresponding to the frequencies $\omega_1, \omega_2, \omega_3$ and ω_4 specified by vertical lines in Fig. 1c. The algorithm for selecting these points is described below in Section 4.

For calibration, we conducted a series of numerical experiments, in which the input pulse's peak power was varied in the range of 0.9–1.26, and the duration – in the range of 0.8–1.15 relative to their initial values. Figure 2 shows the ratio $s_{\text{L}} = S_1/S_2$ of spectral intensities at the selected points of the spectrum depending on the ratio $(p/\tau)^{-1}$. Here p/τ is the ratio of the peak power to the pulse duration, normalised to the unperturbed value, $p = P_{\text{peak}}/P_{\text{peak0}}$, $\tau = T/T_0$; and P_{peak0} and T_0 are the peak power and duration of the unperturbed pulse. It turned out that the dependence of the logarithm of the ratio s_{L} on the parameter τ/p is well approximated by a straight line for virtually all values of P_{peak} and T_0 in the selected parameter region. This confirms our initial assumption that it is the ratio of the peak power to the pulse duration that determines the wing lengths of the broadened spectrum. Using linear regression, we found the coefficients $h = -4.931$ and $q = 3.516$ in the approximation

$$\ln s = h(\tau/p) + q, \tag{4}$$

which was further used in numerical experiments.

In order to simulate a situation close to the conditions of real experiments, we tried to restore the signal parameters with random perturbations. In a typical situation, the pulse at the output of laser systems has an asymmetric envelope shape,

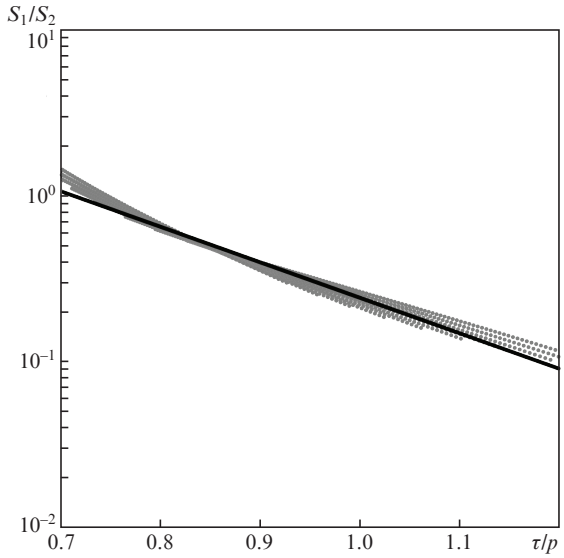

Figure 2. Ratio of spectral intensities, S_1/S_2, as a function of the normalised ratio τ/p obtained by numerical simulation for different durations and peak powers of the input probe pulse (grey dots), and the exponential function approximating this dependence (solid line).

a nonzero phase (for example, due to detuning of the stretcher–compressor system), and may also contain a fairly extended pedestal with a noticeable energy. To take into account these factors, we set the disturbed pulse shape in the form:

$$A(t) = A\exp\{-[t + f(t)]^2/T_0^2 + i\phi(t)\} + D\exp[-(t - t_{pd})^2/T_{pd}^2]. \quad (5)$$

Here $f(t)$ is a function defining the temporal distortion of the pulse shape (including duration variation and asymmetry); $\phi(t)$ is a function defining the pulse phase distortion; D is the pulse pedestal amplitude; T_{pd} is the pedestal duration; and t_{pd} is the pedestal shift relative to the main pulse. The function $f(t)$ is a piecewise linear function with a segment length of $0.8T_0$ и and a slope of segments given by uniformly distributed random numbers in the range $-0.25 \div 0.25$. This function introduces random variations into the main pulse duration and generates its asymmetry.

The amplitudes of the main pulse (A) and pedestal (D) were given by uniformly distributed random numbers within the ranges of 0.95–1.05 and $-0.7 \div 0.7$, respectively. The duration and shift of the pedestal were constant: $T_{pd} = 5T_0$, $t_{pd} = 0.5T_0$. The resulting normalised peak pulse power fluctuated around an average value of 1 in the range 0.7–1.35 (standard deviation was 0.158). Phase distortions were determined using the function $\phi = \beta_2 t^2 + \beta_3 t^3$, where β_2 and β_3 are random numbers uniformly distributed in the ranges $(-0.3 \div 0.3)T_0^{-2}$ and $(-0.09 \div 0.09)T_0^{-3}$, respectively. A total of 10000 distorted pulse realisations were simulated. The normalised pulse energy fluctuated within significant limits: 0.09–0.27 (average value was 0.15, standard deviation was 0.038). Several characteristic shapes of the pulse and its initial and broadened spectra are shown in Fig. 3. The nonlinearly broadened spectrum acquires a noticeable asymmetry, and its width fluctuates significantly. Nevertheless, in general, the characteristic shape of the spectrum, and in particular the shape of its wings, remains similar to the shape of the unperturbed pulse's wings.

For each simulated spectrum, an algorithm for retrieving the $(p/\tau)_r$ ratio was used, and the exact values p/τ of this ratio were also calculated. To account for the pulse asymmetry, we separately calculated the $(p/\tau)_L$ and $(p/\tau)_H$ ratios based on information regarding the low-frequency and high-frequency wings of the spectrum. The resulting ratio $(p/\tau)_r$ was calculated as the harmonic mean: $(p/\tau)_r = 2[(p/\tau)_L^{-1} + (p/\tau)_H^{-1}]^{-1}$. With this choice of the averaging method, the best results were attained. The data of the numerical experiment are shown in Fig. 4. It can be seen that the exact and restored values correspond quite well to each other – all points on the plot lie near the straight line with a slope coefficient of 1.0047, the correlation coefficient being 0.959. The standard deviation of the restored $(p/\tau)_r$ value from the exact (p/τ) value was 0.042. The result obtained confirms the possibility of using our algorithm to restore the ratio of the peak pulse power to the pulse

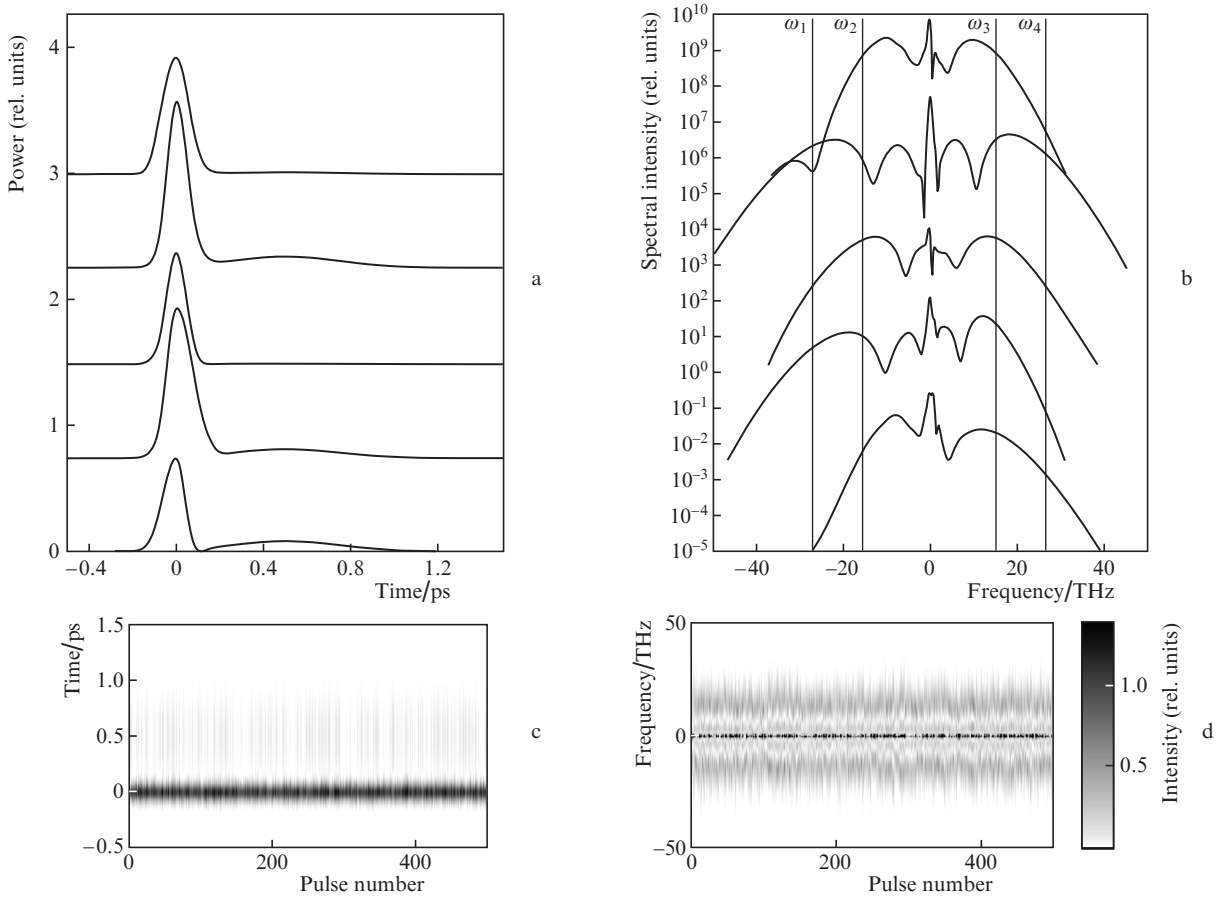

Figure 3. (a) Several realisations of the power profile of perturbed pulses and (b) their corresponding broadened spectra used in the numerical study (for clarity, the power profiles are shifted along the vertical axis by 1.5 rel. units, and the spectra are shifted by 20 dB), as well (c) power profiles and (d) broadened spectra for 500 pulse realisations.

duration from measurements at only four wavelengths of the spectrum broadened due the SPM effect. It should be noted that the presence of both a pedestal containing a significant part of energy and introducing additional asymmetry and not large quadratic and cubic phases of the initial pulse does not significantly impair the results of the p/τ ratio restoration, which gives grounds for the application of our method in real experiments.

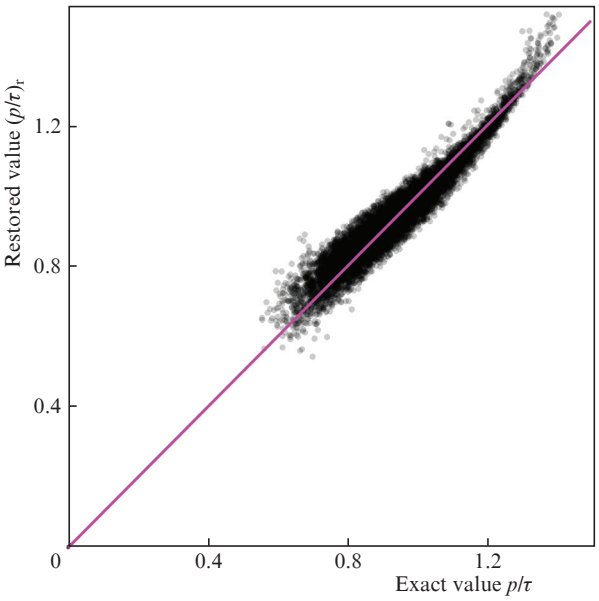

Figure 4. Ratios $(p/\tau)_r$ restored in the numerical experiment vs. exact ratio p/τ for 10000 pulse realisations with random distortions (grey dots) and linear approximation (solid line).

One of the limitations of the method under consideration is that the spectrum broadening within a nonlinear element should occur without significant distortion of its temporal shape, i.e. the contribution of dispersion effects within the limits of the nonlinear element length should be small. The following criterion can be used for evaluation: $\delta_2 L \Delta\omega \ll T$, where δ_2 is the coefficient of quadratic dispersion, L is the nonlinear element length, and $\Delta\omega$ is the broadened spectrum's width. In addition, for the application of our method, the above assumptions regarding the pulse shape must be valid. The presence of small-scale modulation on the broadened spectrum's wings is an indicator that these assumptions are not fulfilled.

4. Experimental results

We used the proposed method in an experiment, the scheme of which (see Fig. 5, a) is based on a fibre laser system with a high-power chirped-pulse amplifier and a grating compressor. The laser system represents an upgraded version of the system described in [13]. The system generates radiation pulses with a centre wavelength of 1.56 μm and a maximum energy up to 10 mJ at a repetition rate of 200 kHz. The duration of a pulse compressed in a compressor on transmitting diffraction gratings is about 0.6 ps. The method we developed was used to monitor the stability of the pulse parameters. With this aim in view, a small part of radiation (with a pulse energy of 50 nJ) is split off and focused into a 2-cm-long nonlinear fibre segment. The nonlinear fibre has a rather thin single-mode core heavily doped with germanium oxide. The fibre dispersion at a wavelength of about 1.55 μm is normal (-20 ps nm^{-1} km^{-1}) which excludes the development of modulation instability and soliton effects. The small fibre length ensures a radiation propagation regime, in which the main effect is the spectrum broadening due to SPM. Dispersion spreading of a pulse is negligible, which was verified by numerical simulation of the pulse propagation, based on the nonlinear Schrödinger equation. The scheme tuning was reduced to optimisation of the radiation input into the nonlinear fibre to attain maximum spectrum broadening.

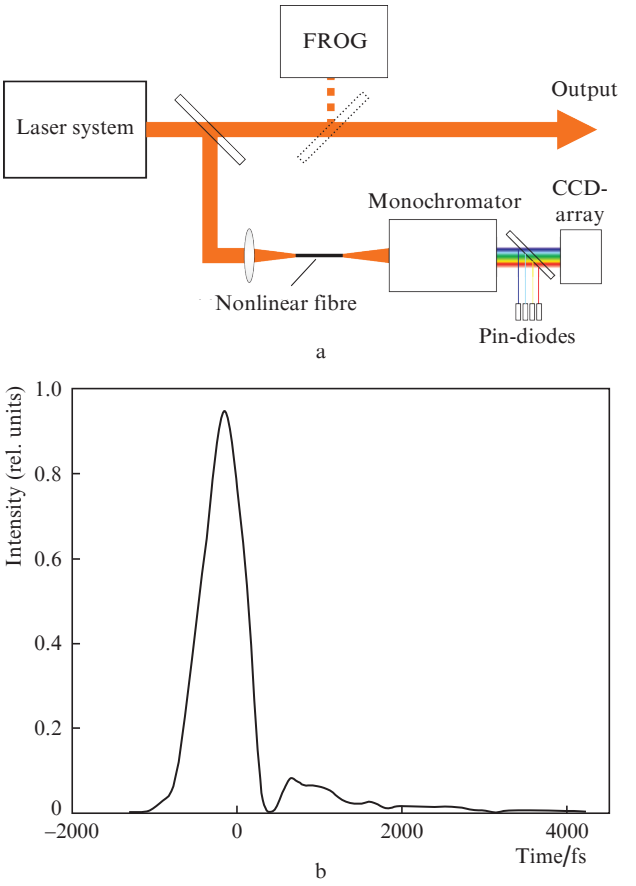

Figure 5. (a) Schematic of the experimental setup and (b) averaged pulse shape at the laser system output, measured by the FROG method.

The broadened pulse spectrum was recorded using a monochromator and a linear InGaAs CCD sensor. The sensor speed was sufficient to record the spectrum in the single-pulse regime at a low pulse repetition rate (200 kHz). In addition, for individual wavelengths, the spectral intensity could be recorded using single-element detectors, i.e. fast pin-photodiodes. Figure 6 shows several spectra measured in the single-pulse regime, and the initial pulse's spectrum. It is seen that the spectrum broadening is quite strong, and a shape typical of the self-modulation process is observed, with the spectrum width fluctuating noticeably from pulse to pulse, which indicates non-ideal stability of the laser system pulses. To apply our method to measuring fluctuations of the p/τ ratio, four points on the spectrum wings were selected, marked by vertical lines in Fig. 6.

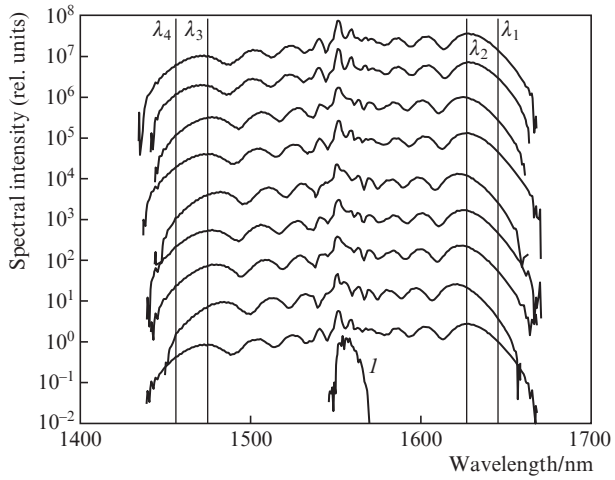

Figure 6. Spectrum at the laser system output (*1*) and examples of the spectra broadened in a nonlinear fibre (for clarity, the spectra are shifted along the vertical axis by 10 dB). Vertical lines indicate the wavelengths λ_{1-4} used to record the spectral intensity on the wings of the broadened spectrum.

The algorithm for selecting the points at which spectral intensities are recorded is as follows. It is necessary to measure the averaged spectrum shape and collect, if possible, statistics on the spectra measured in the single-pulse regime. A typical spectrum broadened due to SPM has an oscillating structure in which the number of peaks increases with increasing nonlinearity. For successful application of our method, the points should be selected on the spectrum wings beyond the extreme maxima, i.e. ω_1, $\omega_2 < \omega_{m1}$, and ω_3, $\omega_4 > \omega_{m2}$, where ω_{m1} and ω_{m2} are frequencies corresponding to the lowest and highest frequency maxima, respectively. At the same time, a too strong shift of the selected frequencies relative to the frequencies corresponding to the spectrum maxima is undesirable due to a decrease in the signal-to-noise ratio. In the experiment, we chose the frequencies ω_2 and ω_3 so that they lie close to the frequencies corresponding to the extreme maxima in the spectrum, while the frequencies ω_1 and ω_4 were chosen so that the characteristic ratios S_1/S_2 and S_4/S_3 were of the order of 0.1.

The position of single-element detectors was adjusted by moving them transverse the beam that was decomposed into a spectrum after the monochromator. The beam passed through the monochromator was blocked at points corresponding to the frequencies $\omega_1,\omega_2,\omega_3$ and ω_4 using a set of thin wires, the spectrum being measured using a pre-calibrated CCD array. Photodetectors were installed in positions corresponding to the blocked parts of the spectrum. The dependence of photodiode sensitivity on the wavelength was taken into account by multiplying the photodiode signal by a calibration factor.

A further algorithm involves calibrating the response to fluctuations of the pulse parameters of the ratio of spectral intensities. The calibration assumes taking into account the characteristic pulse shape that should be measured by one of the available methods. In our experiment, the averaged pulse shape was measured by the FROG method (Fig. 5b). Then, numerical simulation of the spectrum broadening was performed according to expression (2), with the pulse shape taken from the measurements by the FROG method. The average nonlinearity value corresponding to the *B*-integral value equal to 29 was chosen so that the simulated spectrum was most similar to the characteristic spectrum at the fibre output; in this case, the position of extreme maxima in the broadened spectrum was primarily monitored. To determine the coefficients in the approximating formula (4), we numerically simulated the spectrum broadening for *B*-integral values lying in the range of 26–32. These coefficients were found in the same way as in the numerical experiment, and amounted to $h = -4.7$, $q = 3.6$.

In addition, in the numerical experiments employing input pulses of slightly different shapes obtained in several implementations taken from measurements performed by the FROG method, we ascertained that inaccurate knowledge of the input pulse shape does not prevent us from finding the characteristic values of the required coefficients. Verification of the calibration was carried out with a controlled decrease in the signal power at the fibre input and preservation of its duration using a filter with variable optical density, and also with subsequent comparison of the measured spectra with those calculated numerically.

The p/τ ratio values reconstructed using our method for experimental measurements of 48 consecutive pulses are shown in Fig. 7a. This figure also shows values of the total pulse energy measured by a separate detector. It is of interest to note that, in the experiment, the p/τ ratio turned out anticorrelated with the total pulse energy, which, at first glance, seems counterintuitive. However, this can be explained by the fact that nonlinear distortions in the fibre amplifier increase with increasing energy, which leads to a deterioration in the pulse compression.

If we assume that the pulse energy is associated with its duration and peak power by the relation $W = P_{peak}T$, then the duration and peak power of the disturbed pulse can be expressed in terms of the experimentally restored p/τ value and the measured energy W:

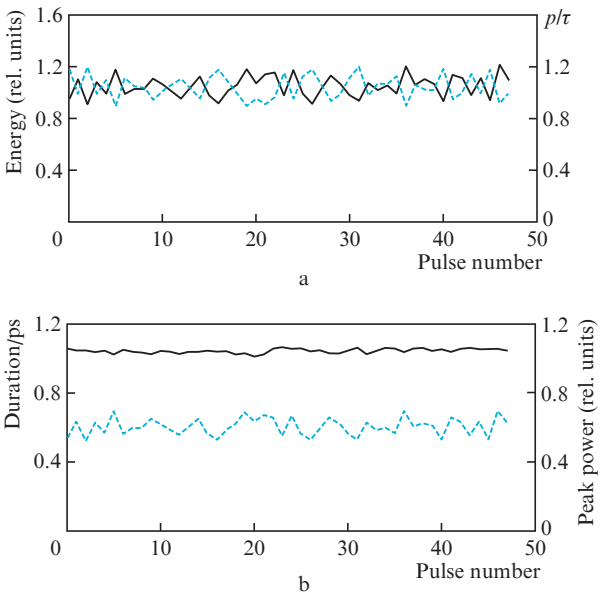

Figure 7. (a) Measured energy normalised to an average value (solid curve) and normalised ratio p/τ restored from spectral measurements for 48 consecutive pulses (dashed curve), as well as (b) duration (dashed curve) and the peak power normalised to an average value (solid curve), both estimated by formula (6).

$$T = T_0\sqrt{\frac{W}{(p/\tau)\,W_0}}, \quad P_{\text{peak}} = P_{\text{peak0}}\sqrt{\frac{(p/\tau)\,W}{W_0}}, \qquad (6)$$

where W_0 is the unperturbed pulse energy. The parameter values obtained from these considerations for our experiment are shown in Fig. 7b. It is seen that the pulse duration correlates with the energy change (Fig. 7a), while the peak power remains virtually unchanged.

Thus, provided that the p/τ ratio and the pulse energy are anticorrelated, the peak pulse power varies slightly, and energy fluctuations are caused by the fluctuations of the pulse duration. This situation can be implemented in the presence of strong nonlinear distortions in the chirped-pulse amplifier. In the case of energy and peak power fluctuations of the uncompressed pulse, the nonlinear phase modulation of the pulse in the amplifier also fluctuates. As the energy increases, the nonlinear phase modulation also increases and the pulse compression deteriorates, so that the compressed pulse duration increases, while its peak power varies slightly. It should be noted that the assumption that the pulse energy is determined by the product $P_{\text{peak}}T$ is, generally speaking, not always true, since the pulse may have a long low-intensity pedestal containing a significant energy fraction. Therefore, in addition to increasing the compressed pulse duration with an increase in its energy, it is possible to increase the energy fraction in the uncompressed pulse's pedestal at the compressor output. Our reasoning is also supported by the fact that, with a purposeful increase in the pump power of the output amplifier, the width of the broadened spectrum decreased on the average, whereas the narrow peak at a wavelength of about 1.56 μm, corresponding, in our opinion, to the uncompressed pedestal, became higher. With a small decrease (by about 10%) in the pump power, the spectrum was broadened, and with its further decrease, the spectrum width gradually decreased.

Elucidation of the specific mechanism responsible for the anticorrelation of the p/τ ratio and the pulse energy, observed in our experiment, is beyond the scope of this work.

5. Discussion

In this paper, we have experimentally demonstrated the applicability of the method we have proposed for pulses with a not very high repetition rate (0.2 MHz). Nevertheless, this method can also be used for pulse sequences with a much higher repetition rate [14], being, in fact, only limited by the speed of photodiodes and the recording system. It should be noted that the measurements can be processed in real time using analogue circuitry even without the digitisation of signals. To perform mathematical operations envisaged by the algorithm, it is necessary to calculate the logarithm of the ratio of photodiode signals, which is equivalent to the difference in the logarithms of the signals and can be done using logarithmic amplifiers and a differential amplifier. Next, it is necessary to perform multiplication by a constant and summation, which can also be done using linear amplifiers.

The opportunity to directly obtain an analogue signal without digital processing opens up broad prospects for the application of our algorithm in feedback systems. By using the developed method to study the ultrahigh frequency sequences of pulses in which the peak intensities and pulse energies are very small, the spectrum can be broadened with the use of highly nonlinear media, for example, soft glass fibres (tellurite, chalcogenide), and the Kerr nonlinearity coefficient of which is several orders of magnitude higher. In addition, the use of soft glasses transparent in the long-wavelength spectrum region makes it possible to use our method for the mid-IR range being insufficiently mastered in terms of generation and measurement of ultrashort pulses.

Despite the fact that, for a large number of tasks, the peak power and duration values separately are of interest, their ratio in many cases may also contain sufficient information about the system. Apparently, our method can be directly applied in fast-feedback systems to stabilise the laser system parameters. In addition, if there is additional information about the pulse, it is possible to separately retrieve the peak power and duration. In particular, if it is known that the entire energy is concentrated in a pulse, and the pedestal energy is negligible, then an additional pulse energy measurement, which can readily be performed in real time, facilitates the calculation of P_{peak} and T values. In a more complex case, additional information can be obtained from measurements based on the use of another type of nonlinearity, for example, by measuring the energy or spectrum of the second harmonic of the signal under study. In our opinion, the development of methods for fast measurement of pulse parameters, based on the joint use of various types of nonlinearity, is very promising.

6. Conclusions

A method of ultrafast evaluation of fluctuations of the ratio of the peak power P_{peak} and the duration T of ultrashort pulses is proposed, based on the measurement of a spectrum nonlinearly broadened in a Kerr nonlinear medium for only four wavelengths. The method ensures a fairly simple measurement processing which can be performed in real time using analogue circuitry even without digitisation of signals; in this case, the speed is only limited by the response time of photodetectors and analogue circuits. Numerical studies have shown the possibility of employing the method even for pulses having significant asymmetry and containing a significant pedestal. The application of the developed method to study fluctuations of the pulse parameters of a high-power laser system was experimentally demonstrated, with a short optical fibre section used for spectrum broadening.

Acknowledgements. This work was supported by the Russian Science Foundation (Project No. 17-72-10236).

References

1. Fu W., Wright L.G., Sidorenko P., Backus S., Wise F.W. *Opt. Express*, **26**, 9432 (2018).
2. Feehan J.S., Price J.H., Butcher T.J., Brocklesby W.S., Frey J.G., Richardson D.J. *Appl. Phys. B*, **123** (1), 43 (2017).
3. Udem T., Holzwarth R., Hänsch T.W. *Nature*, **416** (6877), 233 (2002).
4. Pile B.C., Taylor G.W. *J. Lightwave Technol.*, **30**, 1299 (2012).
5. Walmsley I.A., Dorrer C. *Adv. Opt. Photon.*, **1**, 308 (2009).
6. Klenke A., Müller M., Stark H., Kienel M., Jauregui C., Tünnermann A., Limpert J. *IEEE J. Sel. Top. Quantum Electron.*, **24** (5), 1 (2018).
7. Anashkina E.A., Ginzburg V.N., Kochetkov A.A., Yakovlev I.V., Kim A.V., Khazanov E.A. *Sci. Rep.*, **6**, 33749 (2016).
8. Anashkina E.A., Andrianov A.V., Koptev M.Y., Kim A.V. *IEEE J. Sel. Top. Quantum Electron.*, **24** (3), 1 (2018).
9. Andrianov A.V., Kim A.V., Khazanov E.A. *Quantum Electron.*, **47** (3), 236 (2017) [*Kvantovaya Elektron.*, **47** (3), 236 (2017)].

10. Bobkov K. et al. *Opt. Express*, **25**, 26958 (2017).
11. Wetzel B., Stefani A., Larger L., Lacourt P.A., Merolla J.M., Sylvestre T., Kudlinski A., Mussot A., Genty G., Dias F., Dudley J.M. *Sci. Rep.*, **2**, 882 (2012).
12. Ryczkowski P., Närhi M., Billet C., Merolla J.M., Genty G., Dudley J.M. *Nat. Photonics*, **12** (4), 221 (2018).
13. Kotov L.V., Koptev M.Yu., Anashkina E.A., Murav'ev S.V., Andrianov A.V., Bubnov M.M., Ignat'ev A.D., Lipatov D.S., Gur'yanov A.N., Likhachev M.E., Kim A.V. *Quantum Electron.*, **44** (5), 458 (2014) [*Kvantovaya Elektron.*, **44** (5), 458 (2014)].
14. Andrianov A.V., Myl'nikov V.M., Koptev M.Yu., Murav'ev S.V., Kim A.V. *Quantum Electron.*, **46** (4), 387 (2016) [*Kvantovaya Elektron.*, **46** (4), 387 (2016)].